



The influence of D-lactide content, high-temperature drawing, and blending with poly(butylene adipate-co-terephthalate) elastomer on the physical aging kinetics and ductility of poly(lactic acid)

Gergely Csézi^{1,2} · Tamás Tábi¹

Received: 21 May 2025 / Accepted: 13 May 2026
© The Author(s) 2026

Abstract

In this paper, we investigated the effect of D-lactide content, high-temperature drawing, and blending with poly(butylene adipate-co-terephthalate) (PBAT) on the physical aging kinetics of poly(lactic acid) (PLA), and its morphology, mechanical properties, and phase structure. As PLA is only tough for 1 or 2 h after processing, or after being heated above the glass transition temperature and back, it is crucial to know how we can avoid, or at least slow down, the kinetics of physical aging. Toughening elastomers, in this case, PBAT, can also influence this. PBAT also works as a nucleating agent and so it slows down physical aging; therefore, it toughens PLA not only through increasing its elongation at break and inhibiting crack propagation. We also investigated the influence of the phase structure of the blend on ductility, with a ball-burst test and a scanning electron microscopy (SEM).

Keywords Biopolymer · Poly(lactic acid) · Physical aging · Toughening

Introduction

Physical aging is a phenomenon that occurs in a wide range of polymers after processing when the material cools under its glass transition temperature. This affects the polymer's mechanical, morphological, and other physical properties but not its chemical properties [1, 2]. Tensile strength and tensile modulus increase, but elongation at break and ductility decrease. The effect of physical aging can be reversed by heating the polymer above the glass transition temperature (T_g) and cooling it down again. Then, the process starts over again, so it is a thermally reversible process [2–4]. In many cases, researchers found a connection between the physical aging process and the decrease in free volume and its migration [5, 6]. Still, other studies suggest that molecular

motions occur under T_g down to a specific temperature, called β -transition temperature, which is responsible for this aging phenomenon, as the macromolecules are trying to reach a thermodynamic equilibrium by the β motion of the segments. Some of these studies even question the influence of the change in free volume [7–10]. On the other hand, the process of physical aging happens in semicrystalline polymers too, but not only in their amorphous, but also in their crystalline regions [11–17]. The mechanical stretching of a polymer at a temperature higher than T_g increases its molecular orientation, which can also affect physical aging and make the initially rigid polymer ductile in the drawing direction. However, we still don't fully understand whether it is because of the decreasing free volume or the increasing secondary bonds and crystallinity, slowing the motion of the molecules and slowing down relaxation [18–21].

The popular biopolymer poly(lactic acid) (PLA) is also a glassy polymer, which undergoes rapid, significant physical aging after processing, causing its brittleness, which hinders its application in many fields [4, 10, 22–24]. Right after processing, PLA has over 150% elongation at break at room temperature, which decreases to 5–10% in a few hours. Studies have shown that PLA can also become ductile permanently, by stretching it above its glass transition temperature, but under cold crystallization temperature, and then cooling

✉ Tamás Tábi
tabi@pt.bme.hu

¹ Department of Polymer Engineering, Faculty of Mechanical Engineering, Budapest University of Technology and Economics, Muegyetem rkp. 3., Budapest 1111, Hungary

² HUN-REN-BME Research Group for Composite Science and Technology, Muegyetem rkp. 3., Budapest 1111, Hungary

it [25–27]. As PLA can also be described as a copolymer, the ratio of D- and L-lactide could also affect the rate of physical aging. Nevertheless, there are also studies about toughening PLA by blending it with tough biopolymers, but only a few have investigated the possible effect of the second material on the physical aging of the first material [28–34]. In this study, we investigated if D-lactide content, high-temperature drawing, or the toughening agent influenced the physical aging of PLA, and how they affected its mechanical and thermal properties, and how PBAT affected its ductility. We examined this with ball-burst tests and tensile tests.

Experimental

Materials and processing

The extrusion grade PLAs type 2500HP, 4032D, 2003D and 4060D were purchased from Natureworks (Minnetonka, MN) with a D-lactide content of 0.5%, 1.4%, 4.3%, and 12%, respectively. (The D-lactide contents were provided by the manufacturer.) The PBAT (ecoFlex F Blend 1200) was purchased from BASF (Ludwigshafen, Germany). Prior to processing, we physically mixed PLA (4032D) and PBAT pellets in the ratio of 90/10, 80/20, and 70/30 and then dried the mixtures in a hot air drier at 80 °C for 8 h to remove moisture. Then, we compounded the blends with a twin-screw extruder (LabTech LTE 26–44) to make filaments and then pellets. The extruder was equipped with a 26-mm-diameter screw with an L/D ratio of 44. Zone temperatures were set to 190 °C, 190 °C, 185 °C, 185 °C, 185 °C, 180 °C, 180 °C, 180 °C, 175 °C, 175 °C, 175 °C (from die to hopper). Screw rotation speed was 20 min⁻¹. The 0.5-mm-thick sheets were made from all neat PLAs separately and the PLA/PBAT blends with a LabTech LCR 300 film sheet extruder (screw diameter 25 mm, L/D = 30) equipped with a slit die set to a slit distance of 0.8 mm. The temperature of the chill roll was set to 60 °C, and pulling speed was 0.9 m min⁻¹. For the PLA/PBAT blends, the extrusion temperatures were 190 °C, 185 °C, 180 °C, 175 °C, 175 °C (from die to hopper) and screw rotation speed was 54 min⁻¹, while the temperatures were 200 °C, 195 °C, 185 °C, 175 °C, 170 °C for 4060D and 210 °C, 210 °C, 200 °C, 190 °C, 180 °C for the rest. After extrusion, we cut dumbbell-shaped specimens from the sheets and drew the oriented samples with a Hencky rate of 0.12 s⁻¹ to the different draw ratios in a 70 °C heat chamber, after we waited 3 min for the samples to reach 70 °C.

Methods

Scanning electron microscopy was carried out with a JEOL JSM 6380LA (Jeol Ltd., Japan, Tokyo) after the samples

were broken in liquid nitrogen cryogenically parallel to the extrusion and drawing direction and coated with a gold layer.

Thermal and crystallization properties were examined by differential scanning calorimetry (DSC) (TA Instruments Q2000), in modulated mode. The samples were 4–6 mg measured in 50 mL min⁻¹ nitrogen purge gas from 0 to 200 °C or 40 to 70 °C, with a heating rate of 5 °C min⁻¹, modulated with ± 1 °C min⁻¹. We determined the glass transition temperature (T_g), cold crystallization temperature (T_{cc}), the melting temperature (T_m), and the enthalpy of relaxation at glass transition temperature (ΔH_r), cold crystallization (ΔH_{cc}), and melting (ΔH_m). We calculated the crystallinity from the DSC results using Eq. 1:

$$X_c = \frac{\Delta H_m - \Delta H_{cc}}{\Delta H_f \cdot (1 - \alpha)} \cdot 100(\%) \quad (1)$$

where X (%) is the calculated crystallinity, ΔH_m (J g⁻¹) and ΔH_{cc} (J g⁻¹) are the enthalpy of fusion and the enthalpy of cold crystallization, respectively, while ΔH_f (J g⁻¹) is the enthalpy of fusion for 100% crystalline PLA (93.0 J g⁻¹) and α is the ratio of the other phase.

The tensile tests were performed with a Zwick Z005 universal testing machine (Ulm, Germany) equipped with a 5-kN force-measuring cell. Test speed was 5 mm min⁻¹. For the undrawn samples (ISO 527-2 5A), grip-to-grip separation distance was 50 mm. The size of the drawn samples, as well as the grip distances, differed with the draw ratios (DRs): DR1, 5: 33 mm; DR2: 44 mm; DR3: 66 mm; DR4: 88 mm. The original pretest shape of drawn samples was non-standard, shorter and wider for better drawability in the short-stroke chamber and for easier measurement of the cross-sectional dimensions. The tensile tests were performed at room temperature and normal humidity.

Ball-burst tests were also carried out on the Zwick Z005 universal testing machine with a 5-kN force-measuring cell with a ball-burst tester. Ball speed was 50 mm min⁻¹, the diameter of the ball was 19 mm, and the inner diameter of clamping was 25 mm. After the ball-burst tests, we calculated the ductility index (DI) with the following equation:

$$DI = \frac{W_{tot} - W_{F_{max}}}{W_{tot}}$$

where DI is the ductility index, W_{tot} is the total absorbed energy, and $W_{F_{max}}$ is the energy absorbed until the first crack appeared.

Results and discussion

The aging experiments started with the tensile tests of freshly produced PLA sheets covering all the D-lactide range (0.5%, 1.4%, 4.3% and 12%) in the extrusion grade.

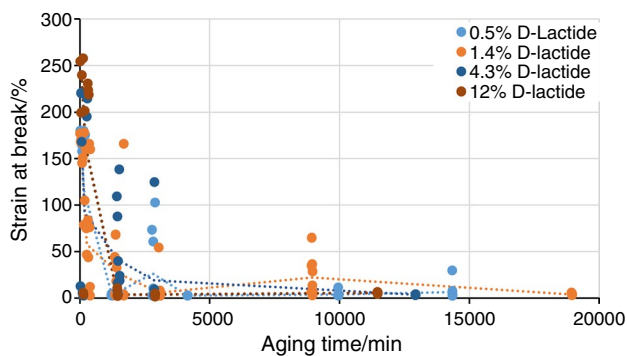


Fig. 1 Strain at break values for the PLA samples with different D-lactide contents as a function of time elapsed after extrusion

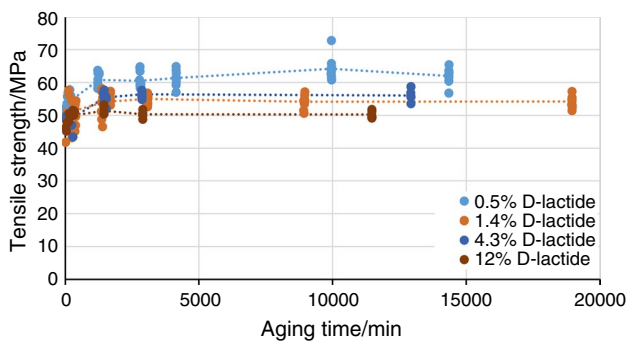


Fig. 2 Tensile strengths of the PLA samples with different D-lactide contents as a function of time elapsed after extrusion

The most significant change happened with the strain at break results from the tensile properties, from 170 to 250% to around 10%, while tensile strength only changed 10% in time. As physical aging is a time-dependent process, the results are presented in the diagram as a function of time elapsed after processing, and individually with average lines in Fig. 1.

The rigid PLA right after the process has a 170–250% elongation at break, depending on its D-lactide content. The higher the content, the higher elongation at break, but the first samples that had permanently reached the ~5–10% strain at break were the samples with the 12% D-lactide content, after one day. The second was the grade with 4.3% D-lactide content; then, the samples with 1.4% and 0.5% D-lactide. Tensile tests indicate that D-lactide content likely affects the speed of physical aging, so the contrast was higher with a higher D-lactide content (Fig. 2).

Tensile tests are a good way of testing how products will behave during use, but for a deeper understanding, the investigation of the morphology is crucial. DSC is a common method of examining physical aging. The relaxation enthalpy around the glass transition temperature (ΔH_r) shows the aging process. The greater the enthalpy, the more

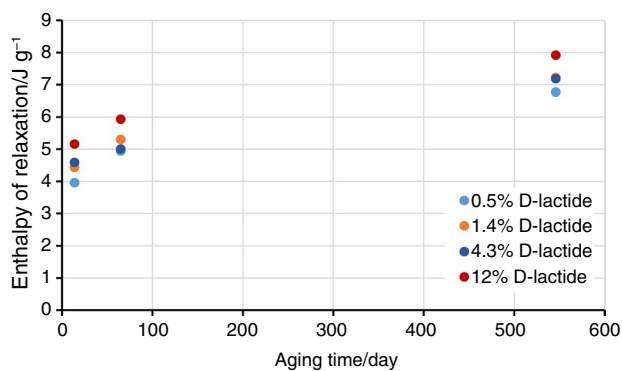


Fig. 3 Relaxational enthalpies of the PLA samples with different D-lactide contents as a function of time elapsed after extrusion

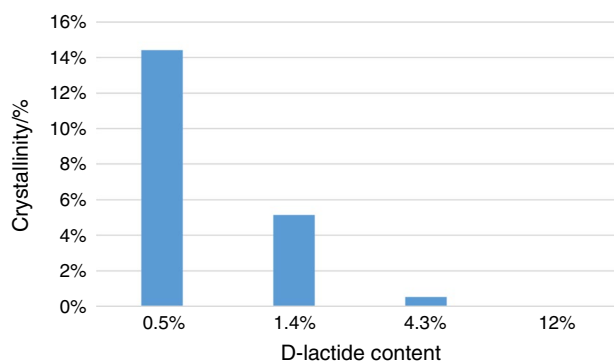


Fig. 4 Crystallinity of the different PLA samples

advanced physical aging is. Therefore, by measuring the different types of PLA samples simultaneously (practically from 0), the difference between their enthalpy shows the speed of aging (Fig. 3).

The measurement results, 2 weeks after the samples were heated above their glass transition temperature and then cooled down (thus physical aging was canceled), showed a very similar order in terms of elongation at break to the tensile test results.

Crystallinity was also measured by DSC (Fig. 4), and as the enthalpy around T_g is mainly attributed to the amorphous phase, specific to the amorphous phase can also provide important data (Fig. 5), even if researchers often connect crystallinity with its slowing effect to physical aging through the physical crosslinking of the macromolecules, which can stop, or at least slow the relaxation of the connected molecules or segments. On the other hand, this should appear in the amorphous phase and segments too.

The specific relaxational enthalpies also show a pattern, which can be connected to the melt flow rate of the samples (Fig. 6), molecular mass and secondary bonding, which is related to D-lactide content.

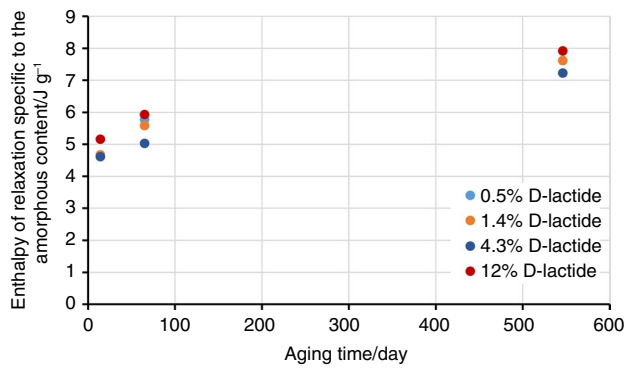


Fig. 5 Relaxational enthalpies of the PLA samples with different D-lactide contents, specific to amorphous content as a function of time elapsed after extrusion

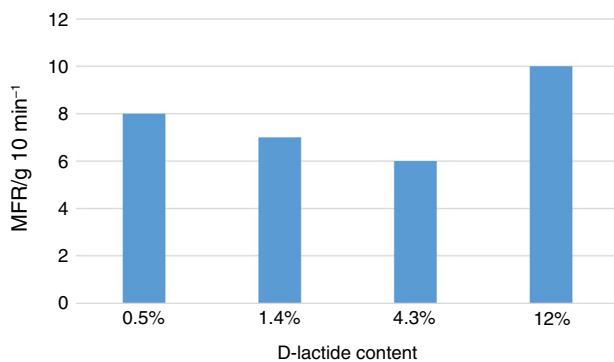


Fig. 6 Melt flow rates of the different PLA grades used, marked with their D-lactide content

It is well known nowadays that drawing PLA at a higher temperature than T_g uniaxially or biaxially significantly increases its toughness, and stretching has a crystal-nucleating effect. This toughness is present in the freshly processed PLA for 1–2 h before physical aging takes place. Now, if that is displayed on the diagram of elongation at break as a function of draw ratio, it is a monotonously decreasing line, without an initial jump (Fig. 7). Therefore, drawing above the glass transition temperature affects physical aging, but does it really stop it, or does it just slow it? Our results indicate that it depends on the draw ratio. At a draw ratio of 1.5, there is no loss after 10 days in elongation at break, but after 260 days, it decreases significantly. On the other hand, if the draw ratio was 2 or above, elongation at break did not change in a 260-day interval. It means that if the PLA is processed, for example, by thermoforming, and the draw ratio reaches 2, its elongation at break increases by an order of magnitude (in the direction of drawing).

Poly(butylene adipate-co-terephthalate) (PBAT) is a biodegradable semicrystalline polyester elastomer, often blended with PLA as a toughening agent, but also works

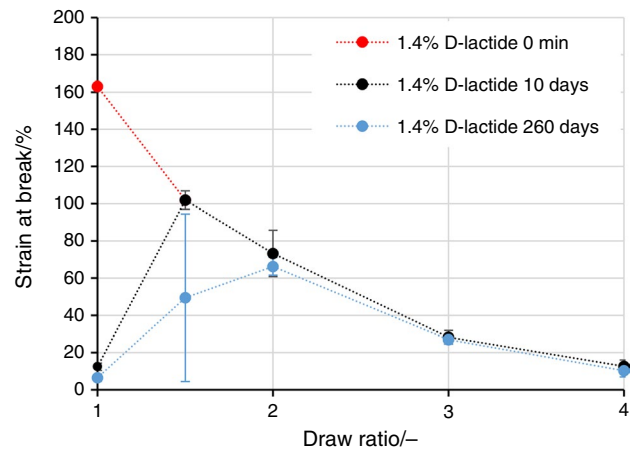


Fig. 7 Strain at break values of the samples containing 1.4% D-lactide as a function of draw ratio, with different elapsed time after processing

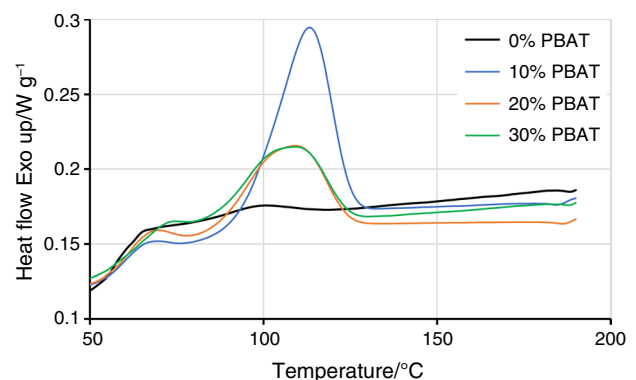


Fig. 8 DSC cooling curves of the different blends

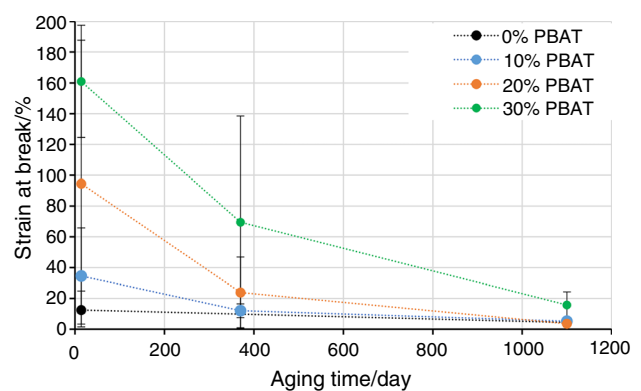


Fig. 9 Strain at break values of the samples with different PBAT contents as a function of days after the process

as a nucleating agent for PLA, which we showed with DSC (Fig. 8).

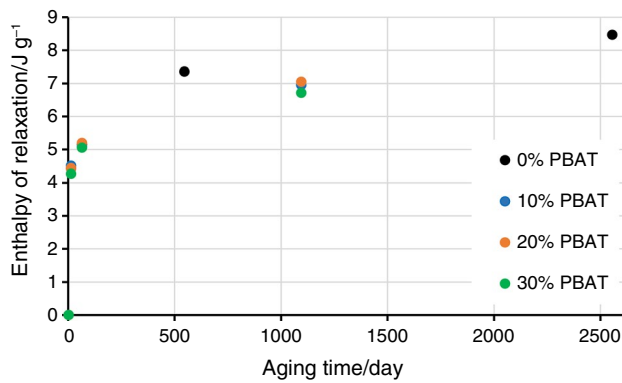


Fig. 10 Relaxational enthalpies of the samples with different PBAT contents as a function of time elapsed after extrusion

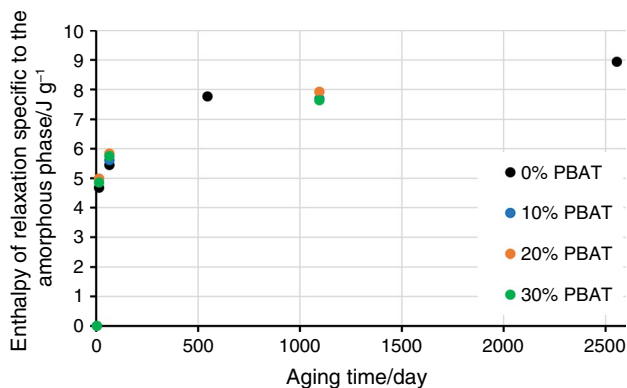


Fig. 11 Relaxational enthalpies of the PLA samples with different PBAT contents specific to amorphous content as a function of time elapsed after extrusion

Making relaxation enthalpy specific to the amorphous content is only one way of investigating the effect of crystallinity, but the number of crystal nuclei may also play a crucial role in the physical aging process. On the other hand, it is possible that PBAT toughens the PLA not only because it is an elastomer, but also because it makes more nuclei and crystallinity and slows the aging process.

Elongation at break values from tensile tests show that undrawn PLA/PBAT blend samples also go through physical aging, but much more slowly (Fig. 9).

That does not mean that the PBAT only toughens PLA through slowing its physical aging and it does not change its fracture behavior through inhibiting crack propagation but in the tensile tests, the former affects necking more.

DSC tests in the two-week interval did not show any significant differences between the neat PLA and the blends when the relaxation enthalpy was only made specific to PLA content, but over a longer time, there are significant differences between them and the speeds of aging differ. In the

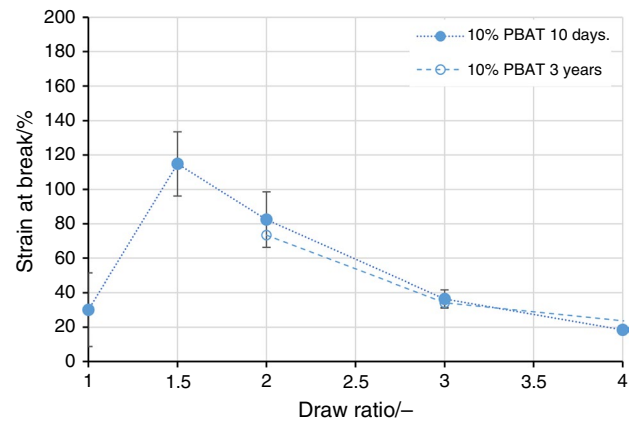


Fig. 12 Strain at break of the samples with 10% PBAT as a function of draw ratio, with different elapsed times after processing

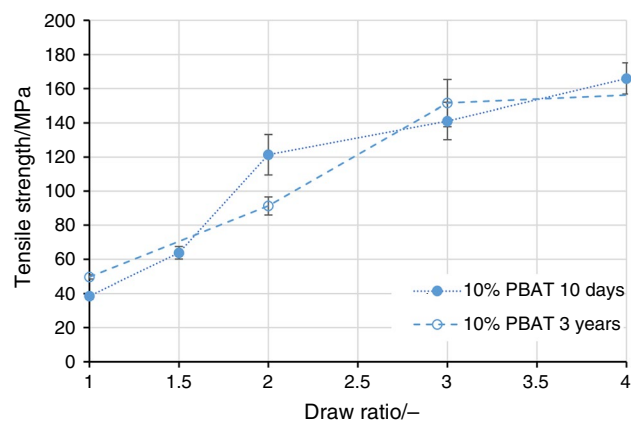


Fig. 13 Tensile strengths of the samples with 10% PBAT as a function of draw ratio, with different elapsed times after processing

range of 10%–30% PBAT content, aging speed decreased with the same amount (Fig. 10).

An opposite phenomenon can be seen after we make the enthalpy specific to the amorphous content. Now in a short time (a few months), the enthalpy of the neat PLA is smaller than that of the blends, which means that physical aging is faster in the amorphous regions of the blends, especially in the PLA phase. However, elongation at break is still much higher, so this may be indirect evidence of how more nuclei can affect the aging process and that the investigation of only the relaxation enthalpy is not enough (Fig. 11).

Uniaxially drawn PBAT samples show the same tendency in elongation at break as the neat 4032D PLA did. At DR2 or higher, elongation at break did not change significantly after three years (Fig. 12).

While elongation at break decreases when the material is drawn uniaxially, tensile strength increases. The changes are

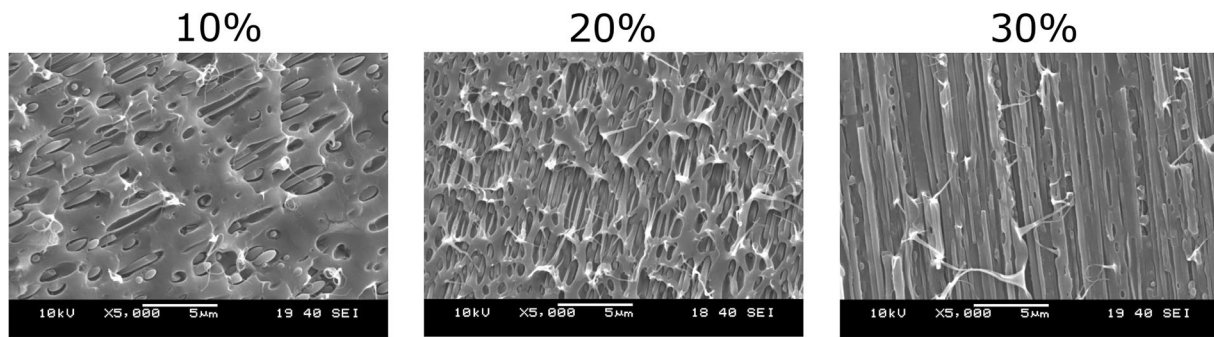
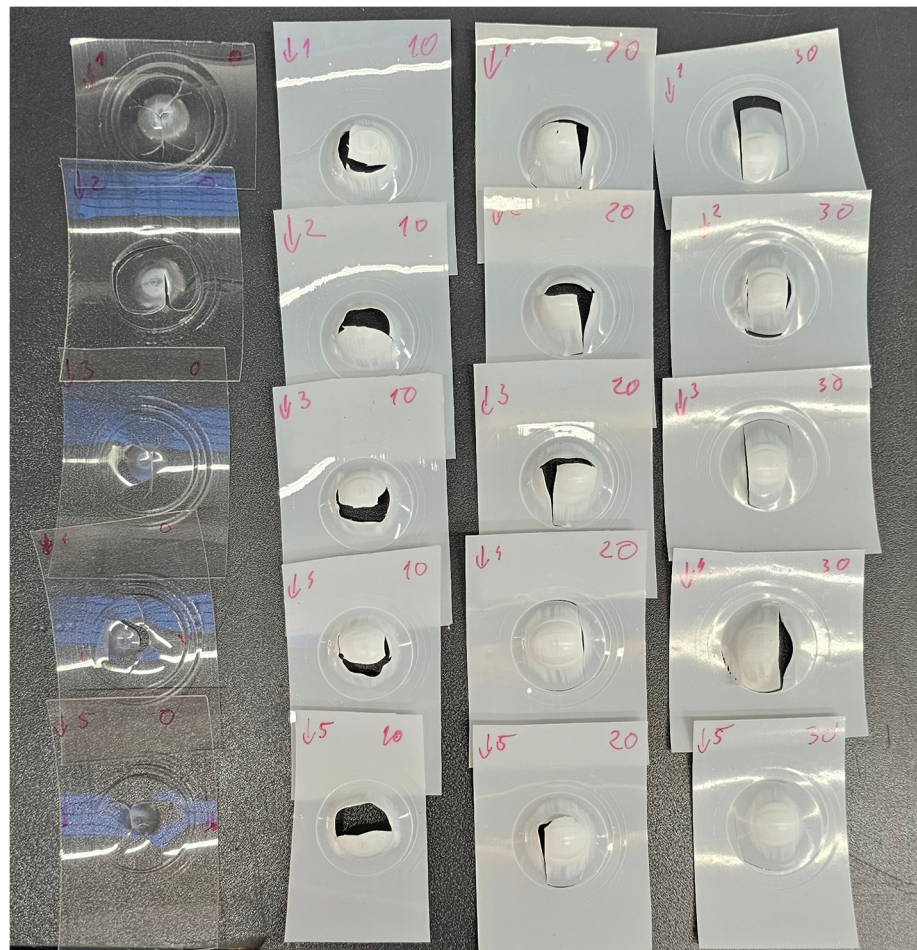


Fig. 14 SEM images of the PLA/PBAT blends containing 10%, 20%, and 30% PBAT

Fig. 15 Ball-burst-tested samples in the order of PBAT content, extrusion direction vertically



insignificant in three years and do not follow any tendency (Fig. 13).

Tensile properties, especially strain at break, were mentioned above, with a side note that PBAT delays physical aging. Also, in time, toughness decreases if calculated from the tensile test. However, in other tests, which directly measure ductility and show the fracture forms, we can check how else PBAT can work on the toughness of

the matrix polymer and what the connection is between the phase structures.

With our process parameter settings, the SEM images from the longitudinal (extrusion direction) cross-sections of the films can be seen in Fig. 14.

The images show that the extrusion samples have phase orientations. At 10% content, the PBAT is in droplets shaped slightly like ellipsoids. At 20%, the phase structure looks like a network, but we did not investigate

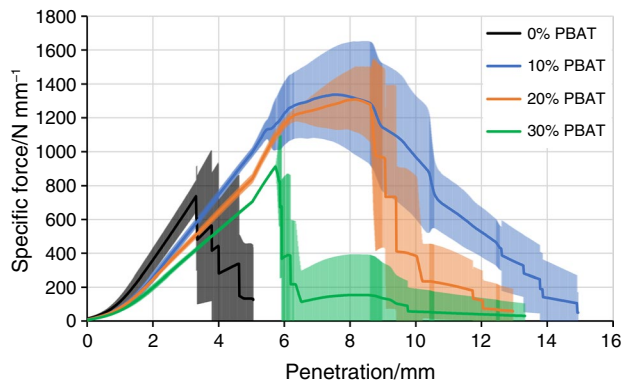


Fig. 16 Average specific force–penetration curves of the ball-burst-tested samples with different PBAT contents

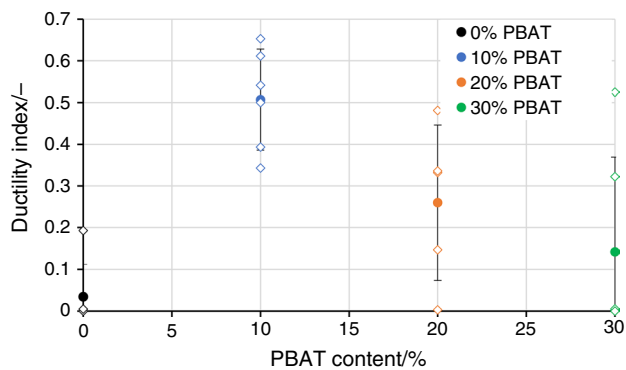


Fig. 17 Ductility indexes as a function of PBAT content

whether there was a co-continuous phase. At 30%, the phase structure was a very oriented network of rods in the matrix. Still, in conclusion, as PBAT content increases, the phase boundary is increasingly in the direction of extrusion and increasingly longer.

After ball-burst tests, the images of the samples show that these oriented phase boundaries drove the fractures and the poor adhesion of the two phases because of the absence of compatibilizers, which was manifested in rigid failure in the extrusion direction (Fig. 15).

The force, specific to the thickness of the sheet, was also different for the different blends during the tests. The stiffness of the blends decreased with increasing amounts of PBAT. However, the highest specific force was measured with the sample with the lowest PBAT content (Fig. 16).

Ductility, shown by the ductility indexes (DI), was also the greatest, when PBAT content was 10%. This means that after the crack appeared, propagation was slow and balanced, but as the phase structure was more oriented with a greater PBAT content, ductility decreased, and after the crack appeared, propagation was getting faster and more and more unbalanced (Fig. 17).

Conclusions

This paper focuses on the physical aging kinetics of poly(lactic acid) (PLA), with special attention to the effect of D-lactide content, drawing above the glass transition temperature and poly(butylene adipate-co-terephthalate) (PBAT) content in PLA/PBAT blends. We have shown that D-lactide content, crystalline fraction, and MFR influence physical aging. When the PLA had crystallinity, physical aging was slower, and as the melt flow rate was smaller, the relaxational enthalpies were also smaller.

Drawing the PLA above the glass transition temperature (T_g) can make PLA tough in the direction of drawing, which tensile tests have shown. This is more lasting toughening, thanks to the large number of crystal nuclei as a result of drawing, which hold together the segments of macromolecules, thus slowing physical aging. If this is not known, it might seem that both the ductility and strength of PLA can be enhanced by drawing uniaxially between the glass transition temperature (T_g) and the cold crystallization temperature (T_{cc}), but in reality, only its strength increases, its elongation at break does not, if we take into account that immediately after it is produced, the elongation at break of PLA can be up to 250% at room temperature and only decreases to around 10% due to aging, in a few hours.

PBAT also enhances crystallinity as a nucleating agent, and our investigation proved that this elastomer toughens PLA in two ways. On the one hand, it slows the kinetic of physical aging, and on the other hand, ductility was best when the PBAT was dispersed in droplets in the matrix, and the phase structure was not oriented, so crack propagation was slow, unoriented, and the crack absorbed more energy, as it lost its sharp edge when it reached a PBAT droplet.

Acknowledgements This work was supported by the National Research, Development, and Innovation Office, Hungary (2019-1.1.1-PIACI-KFI-2019-00335). Project no. TKP-6-6/PALY-2021 has been implemented with the support provided by the Ministry of Culture and Innovation of Hungary from the National Research, Development and Innovation Fund, financed under the TKP2021-NVA funding scheme. As author Tamás Tábi, I would like to thank God for giving me a loving family, wife and son.

Author contributions Gergely Csézi did methodology, measurements; writing—review and editing, and visualization. Tamás Tábi done conceptualization, supervision, writing—original draft, project administration, and funding acquisition.

Funding Open access funding provided by Budapest University of Technology and Economics.

Open Access This article is licensed under a Creative Commons Attribution 4.0 International License, which permits use, sharing, adaptation, distribution and reproduction in any medium or format, as long as you give appropriate credit to the original author(s) and the source, provide a link to the Creative Commons licence, and indicate if changes

were made. The images or other third party material in this article are included in the article's Creative Commons licence, unless indicated otherwise in a credit line to the material. If material is not included in the article's Creative Commons licence and your intended use is not permitted by statutory regulation or exceeds the permitted use, you will need to obtain permission directly from the copyright holder. To view a copy of this licence, visit <http://creativecommons.org/licenses/by/4.0/>.

References

- Hutchinson JM. Physical aging of polymers. *Prog Polym Sci*. 1995;20(4):703–60.
- Volynskii AL, Efimov AV, Bakeev NF. Structural aspects of physical aging of polymer glasses. *Polym Sci, Ser C*. 2007;49(4):301–20.
- Gamez-Perez J, et al. Fracture behavior of quenched poly(lactic acid). *Express Polym Lett*. 2011;5:82–91.
- Pan P, Zhu B, Inoue Y. Enthalpy relaxation and embrittlement of poly(L-lactide) during physical aging. *Macromolecules*. 2007;40(26):9664–71.
- Moynihan CT, et al. Dependence of the fictive temperature of glass on cooling rate. *J Am Ceram Soc*. 1976;59(1–2):12–6.
- Williams G, Watts DC. Non-symmetrical dielectric relaxation behaviour arising from a simple empirical decay function. *Trans Faraday Soc*. 1970;66(0):80–5.
- Struik LCE. Physical aging in amorphous glassy polymers. *Ann N Y Acad Sci*. 1976;279(1):78–85.
- Bailey RT, North AM, Pethrick RA. Molecular motion in high polymers. (No Title). 1981.
- Davis WJ, Pethrick RA. Investigation of physical ageing in polymethylmethacrylate using positron annihilation, dielectric relaxation and dynamic mechanical thermal analysis. *Polymer*. 1998;39(2):255–66.
- Cui L, et al. Physical ageing of poly(lactic acid): factors and consequences for practice. *Polymer*. 2020;186:122014.
- Shafee EE. Effect of aging on the mechanical properties of cold-crystallized poly(trimethylene terephthalate). *Polymer*. 2003;44(13):3727–32.
- Struik LCE. Physical aging in amorphous polymers and other materials. 1978.
- Struik LCE. The mechanical and physical ageing of semicrystalline polymers: 1. *Polymer*. 1987;28(9):1521–33.
- Struik LCE. The mechanical behaviour and physical ageing of semicrystalline polymers: 2. *Polymer*. 1987;28(9):1534–42.
- Struik LCE. Mechanical behaviour and physical ageing of semicrystalline polymers: 3. Prediction of long term creep from short time tests. *Polymer*. 1989;30(5):799–814.
- Struik LCE. Mechanical behaviour and physical ageing of semicrystalline polymers: 4. *Polymer*. 1989;30(5):815–30.
- Spinu I, McKenna GB. Physical aging of nylon 66. *Polym Eng Sci*. 1994;34(24):1808–14.
- Zartman GD, et al. How melt-stretching affects mechanical behavior of polymer glasses. *Macromolecules*. 2012;45(16):6719–32.
- Razavi M, Wang S-Q. Why is crystalline poly(lactic acid) brittle at room temperature? *Macromolecules*. 2019;52(14):5429–41.
- Zheng G, et al. Enhanced strength, toughness and heat resistance of poly(lactic acid) with good transparency and biodegradability by uniaxial pre-stretching. *Int J Biol Macromol*. 2024;278:135222.
- Zhang T, et al. Fabrication of reinforced and toughened poly(lactic acid)/poly(butylene adipate-co-terephthalate) composites through solid die drawing process. *J Appl Polym Sci*. 2020;137(36):49071.
- Cai H, et al. Effects of physical aging, crystallinity, and orientation on the enzymatic degradation of poly(lactic acid). *J Polym Sci, Part B: Polym Phys*. 1996;34(16):2701–8.
- Kwon M, Lee SC, Jeong YG. Influences of physical aging on enthalpy relaxation behavior, gas permeability, and dynamic mechanical property of polylactide films with various D-isomer contents. *Macromol Res*. 2010;18(4):346–51.
- Stefaniak K, Masek A. Poly(lactic acid) (PLA)—short review of synthesis methods, properties, recent progress, and new challenges. *Express Polym Lett*. 2025;19:386–408.
- Chen X, Kalish J, Hsu SL. Structure evolution of α' -phase poly(lactic acid). *J Polym Sci B Polym Phys*. 2011;49(20):1446–54.
- Xu S, Tahon J-F, De-Waele I, Stoclet G, Gaucher V. Brittle-to-ductile transition of PLA induced by macromolecular orientation. *Express Polym Lett*. 2020;14(11):1034–47.
- Chen Y, et al. Impact of d-isomer content on the microstructure and mechanical properties of uniaxially pre-stretched poly(lactic acid). *Polymer*. 2020;186:122022.
- Masa B, Tanrattanakul V, Jaratrotkamjorn R. Synthesis and characteristics of α -carboxylic, ω -hydroxyl natural rubber toughened poly(lactic acid). *Express Polym Lett*. 2023;17:1121–34.
- Pouriman H, et al. Mechanical, thermal and rheological investigation of poly(lactic acid)(PLA)/poly(3-hydroxybutyrate-co-hydroxyvalerate) (PHBV) blend within its synergistic elongation effect region. *Express Polym Lett*. 2023;17:373–89.
- Pouriman H, Graham K, Jayaraman K. Monolayer films from poly(lactic acid) PLA/poly(3-hydroxybutyrate-co-hydroxyvalerate) PHBV blends for food packaging applications. *Express Polym Lett*. 2023;17:1007–18.
- Chen K, et al. Physical aging-induced embrittlement of PLA/PBAT blends probed by tensile test and AFM nanomechanical mapping. *Mater Lett*. 2022;326:132938.
- Aversa C, et al. Compatibilization strategies and analysis of morphological features of poly(butylene adipate-co-terephthalate) (PBAT)/poly(lactic acid) PLA blends: a state-of-art review. *Eur Polym J*. 2022;173:111304.
- Deng Y, et al. Optimising ductility of poly(Lactic acid)/poly(butylene adipate-co-terephthalate) blends through co-continuous phase morphology. *J Polym Environ*. 2018;26(9):3802–16.
- Su S, Duhme M, Kopitzky R. Uncompatibilized PBAT/PLA blends: manufacturability, miscibility and properties. *Materials*. 2020;13(21):4897.

Publisher's Note Springer Nature remains neutral with regard to jurisdictional claims in published maps and institutional affiliations.